PL-TR-93-2118

WAVE PROPAGATION NEAR EXPLOSIVE SOURCES

Lane R. Johnson

Seismographic Station
University of California
Berkeley, CA 94720

20 May 1993

Scientific Report No. 2

PHILLIPS LABORATORY
Directorate of Geophysics
AIR FORCE MATERIEL COMMAND
HANSCOM AIR FORCE BASE, MA 01731-3010

The views and conclusions contained in this document are those of the authors and should not be interpreted as representing the official policies, either expressed or implied, of the Air Force or the U.S. Government.

This technical report has been reviewed and is approved for publication.

JAMES F. LEWKOWICZ
Contract Manager
Solid Earth Geophysics Branch
Earth Sciences Division

JAMES F. LEWKOWICZ
Branch Chief
Solid Earth Geophysics Branch
Earth Sciences Division

DONALD H. ECKHARDT, Director
Earth Sciences Division

This document has been reviewed by the ESD Public Affairs Office (PA) and is releasable to the National Technical Information Service (NTIS).

Qualified requestors may obtain additional copies from the Defense Technical Information Center. All others should apply to the National Technical Information Service.

If your address has changed, or if you wish to be removed from the mailing list, or if the addressee is no longer employed by your organization, please notify PL/IMA, 29 Randolph Road, Hanscom AFB MA 01731-3010. This will assist us in maintaining a current mailing list.

Do not return copies of this report unless contractual obligations or notices on a specific document require that it be returned.

REPORT DOCUMENTATION PAGE

Form Approved
OMB No. 0704-0188

1. AGENCY USE ONLY (Leave blank)	2. REPORT DATE	3. REPORT TYPE AND DATES COVERED
	20 May 1993	Scientific No. 2

4. TITLE AND SUBTITLE
Wave Propagation Near Explosive Sources

5. FUNDING NUMBERS
PE 62101F
PR 7600 TA 09 WU BF
Contract F19628-90-K-0055

6. AUTHOR(S)
Lane R. Johnson

7. PERFORMING ORGANIZATION NAME(S) AND ADDRESS(ES)
University of California
Seismographic Station
Berkeley, CA 94720

8. PERFORMING ORGANIZATION REPORT NUMBER

9. SPONSORING/MONITORING AGENCY NAME(S) AND ADDRESS(ES)
Phillips Laboratory
29 Randolph Road
Hanscom AFB, MA 01731-3010
Contract Manager: James Lewkowicz/GPEH

10. SPONSORING/MONITORING AGENCY REPORT NUMBER
PL-TR-93- 2118

11. SUPPLEMENTARY NOTES

12a. DISTRIBUTION/AVAILABILITY STATEMENT
Approved for public release;
Distribution unlimited

12b. DISTRIBUTION CODE

13. ABSTRACT *(Maximum 200 words)*

A basic goal of seismic yield estimation is to understand the relationship between the yield of an explosion and the amplitude of seismic waves radiated into the far field. Of particular interest in this relationship is the role played by material properties in the vicinity of the source. This study is an attempt to investigate this problem through the use of an equivalent elastic treatment for the region between the original cavity radius and the elastic radius. Equations are developed which allow the material properties to be modified as a function of the level of stress, and a propagator method is presented which solves the elastodynamic equations for a visco-elastic material with properties that vary as a function of radial distance from the explosive source. The relations between parameters measured in laboratory tests and the material properties required in wave propagation problems are also reviewed. While this approach is only an approximation to calculations with hydrodynamic and equation-of-state codes, it has the advantage of providing simple analytic results in which the role of various model parameters is easily investigated.

14. SUBJECT TERMS		15. NUMBER OF PAGES
Wave propagation Nonlinear elastic	Explosive sources	32
		16. PRICE CODE

17. SECURITY CLASSIFICATION OF REPORT	18. SECURITY CLASSIFICATION OF THIS PAGE	19. SECURITY CLASSIFICATION OF ABSTRACT	20. LIMITATION OF ABSTRACT
Unclassified	Unclassified	Unclassified	SAR

Wave Propagation Near Explosive Sources

Lane R. Johnson

Center for Computational Seismology, Lawrence Berkeley Laboratory,

and Seismographic Station, University of California,

Berkeley, California 94720

1. Introduction

The relationship between the energy of an explosive source and the amplitude of the seismic waves which are radiated into the far field has been a primary interest of the verification program since its beginning (Latter et al., 1959). The problem is made difficult by the fact that the seismic energy represents only a small fraction of the total energy. Most of the energy of the explosion is deposited within the elastic radius by a series of complicated non-linear processes. Given that the wave propagation problem beyond the elastic radius is essentially solved, the primary difficulty concerns the treatment of the non-linear region surrounding the source. A number of computer codes have been developed for modeling this region, but they are fairly complicated, involving hydrodynamic effects, shock waves, and non-linear equations of state. Because of the basic numerical approach which is followed in these codes, they do not readily provide insight into questions about which parameters are playing critical roles in determining the radiated elastic waves. This has motivated the investigation of an alternative method of modeling this region immediately surrounding an explosive source.

The basic objective of the research described in this report is to explain the energy that is radiated into the elastic region by an explosive source. The energy which is deposited within the elastic radius is not of direct interest in the sense that it does not propagate as far as the elastic region. However, it is necessary to obtain an estimate of the total amount of this energy which is deposited within the elastic radius, as this must be subtracted from the energy of the explosion in order to determine the energy that reaches the elastic region.

The basic approach being investigated is to use an equivalent elastic treatment for the region between the original cavity radius and the elastic radius. This concept of an equivalent elastic medium has been used quite successfully by earthquake engineers to model the non-linear behavior of soils that occurs during strong ground motion. An advantage of this approach is that it is possible to make use of the analytical solutions which are available for the linear problem. The central idea of the method is to

make the material properties a function of the stress in the outward propagating pressure pulse and obtain the results in the form of a simple numerical propagation of analytical solutions. The present formulation relates density and bulk elastic properties to the peak pressure in the pressure pulse and shear and anelastic properties to the maximum shear stress. The material properties are adjusted in an iterative process so that appropriate values are present in the vicinity of the propagating pressure pulse. While this approach is only an approximation to calculations with hydrodynamic equation-of-state codes, it has the advantage of providing simple analytic results in which the role of various model parameters is easily investigated. This is important when one wants to conduct a sensitivity analysis over a wide range of explosion sizes and material parameters.

There are a number of lines of evidence which suggest that this type of approach could possibly provide some useful results. The study of Denny and Johnson (1991) seemed to indicate that relatively simple scaling relationships could explain a wide variety of explosion data. A single scaling relationship was found to be reasonably successful in reconciling explosion data that spanned a broad range of explosion yield and source medium. The data set also spanned different types of explosions, including nuclear explosions, chemical explosions in the field, and small chemical explosions in the laboratory. These results could be interpreted to mean that, if the explosion data can be explained by simple relationships, then a correspondingly simple treatment of the physics of the problem might also be possible. There are a number of examples in continuum mechanics where a general treatment of a problem which lumps together a number physical mechanisms is possible. Anelastic attenuation of seismic waves is one such example, as the basic physics of the process is not fully understood and it is likely that a number of different processes are responsible, and yet it is possible to describe all of these effects with a single parameter, the quality factor Q. Finally, if this problem is viewed in terms of energy, it becomes a basic transport problem, with the primary task that of determining how much of the energy is absorbed and how much is transported.

2. Equivalent Elastic Method

The region immediately surrounding an explosive source experiences stresses of sufficient magnitude so that, at least temporarily, the material properties are significantly different than in the normal state of low stress. The basic idea of the equivalent elastic method is to retain the assumption of a linear elastic constitutive relationship, but to adjust the elastic constants according to the level of the stress. The process is different for the bulk and shear properties. It should be pointed out that the material being considered here is actually a linear visco-elastic material, as the constitutive equations are assumed to have both elastic and viscous terms.

Consider first the bulk properties. Majtenyi and Foster (1992) have suggested analytical expressions for describing the changes in density and compressional velocity caused by the passage of a one-dimensional pressure wave. These have been modified below to make them more appropriate for the case of waves in three dimensions. Let ρ_u be the ultimate or maximum density and P be the pressure. Then the dependence of density upon pressure is expressed as

$$\rho(P) = \rho_u - (\rho_u - \rho_o)\, e^{-AP} \tag{2.1}$$

where

$$A \equiv \frac{1}{k_o}\frac{\rho_o}{\rho_u - \rho_o} \tag{2.2}$$

and ρ_o and k_o are low pressure values of the density and bulk modulus, respectively. In terms of the low pressure values of the P velocity and S velocity

$$\frac{k_o}{\rho_o} = V_{po}^2 - \frac{4}{3}V_{so}^2 \tag{2.3}$$

The compressional velocity as a function of pressure is given by

$$V_p(P) = \left[V_{po}^2 + \frac{2}{\rho_u}[P + \frac{1}{A}ln(\frac{\rho(P)}{\rho_o})]\right]^{1/2} \tag{2.4}$$

Next consider the shear properties. In this case the shear modulus and the shear quality factor are adjusted according to the shear stress. However, it is convenient to express the relationships in terms of shear strain rather than shear stress. Let τ_{max} be the shear strength, the maximum shear stress that the material will sustain, and define the reference strain by

$$e_r = \frac{\tau_{max}}{\mu_o} \tag{2.5}$$

Here μ_o is the low stress shear modulus, which can be obtained from the low stress shear velocity by

$$\mu_o = \rho_o V_{so}^2 \tag{2.6}$$

The apparent strain associated with the shear stress τ is defined to be

$$e = \frac{\tau}{\mu_o}$$

Then the simple hyperbolic stress-strain relationship (Hardin and Drnevich, 1972b) yields the effective shear modulus

$$\mu(e) = \mu_o \frac{1}{1 + e/e_r} \tag{2.7}$$

Similarly, the effective damping ratio is

$$d(e) = d_{\max} \frac{e/e_r}{1 + e/e_r} \tag{2.8}$$

where $d_{\max}$ is the maximum damping ratio for the material.

A modified hyperbolic relationship can be obtained by defining a hyperbolic strain as

$$e_h = \frac{e}{e_r}\left[1 + a\, e^{-b\frac{e}{e_r}}\right] \tag{2.9}$$

where a and b are material dependent constants. Then

$$\mu(e) = \mu_o \frac{1}{1 + e_h} \tag{2.10}$$

and

$$d(e) = d_{\max} \frac{e_h}{1 + e_h} \tag{2.11}$$

Note that the constants a and b used in defining e_h may be different for the calculation of μ and d.

3. Linear Visco-Elastic Solid

An important aspect of the equivalent elastic treatment as it is being used in this problem is the treatment of energy absorption. This is achieved by treating the material as a linear visco-elastic solid. Because the energy absorption in this problem is quite significant, it is worth reviewing the basic definitions of the quantities involved. The starting point is to assume that the Boltzman principle of superposition can be applied and that the material can be described by a linear hereditary constitutive equation. Then the stress-strain relationship can be written as

$$\tau_{ij}(t) = \int_{-\infty}^{t} C_{ijkl}(t-\gamma)\, de_{kl}(\gamma) \tag{3.1}$$

where $C_{ijkl}(t)$ are now the generalized visco-elastic moduli. In the frequency domain this becomes

$$\tau_{ij}(\omega) = \tilde{C}_{ijkl}(\omega)\, e_{kl}(\omega) \tag{3.2}$$

where the following Fourier transform pair has been introduced

$$\tilde{C}_{ijkl}(\omega) \quad \overset{F}{\longleftrightarrow} \quad \frac{d}{dt} C_{ijkl}(t) \tag{3.3}$$

In order to simplify the algebra, consider only one of the elastic moduli and then the basic hereditary constitutive equation can be written as

$$\tau(t) = \int_{-\infty}^{t} C(t-\gamma)\, de(\gamma) \tag{3.4}$$

In general $\tilde{C}(\omega)$ will be a complex quantity so

$$\begin{aligned} \tilde{C}(\omega) &= \mathrm{Re}\{\tilde{C}(\omega)\} + i\ \mathrm{Im}\{\tilde{C}(\omega)\} \\ &= |\tilde{C}(\omega)|\, e^{i\theta_C} \end{aligned} \tag{3.5}$$

where

$$\tan(\theta_C) = \frac{\mathrm{Im}\{\tilde{C}(\omega)\}}{\mathrm{Re}\{\tilde{C}(\omega)\}} \tag{3.6}$$

This study follows a practice common in seismology and introduces the quality factor Q through the equation (Aki and Richards, 1980).

$$\tilde{C}(\omega) = \mathrm{Re}\{\tilde{C}(\omega)\}(1 + i\ Q^{-1}) \tag{3.7}$$

so that the inverse quality factor is defined as

$$Q^{-1} \equiv \frac{\mathrm{Im}\{\tilde{C}(\omega)\}}{\mathrm{Re}\{\tilde{C}(\omega)\}} = \tan(\theta_C) \tag{3.8}$$

A critical difference between elastic and visco-elastic materials involves the the fact that energy is not conserved for the latter. For a general deformation, the change in internal strain energy is

$$\rho[\varepsilon(t) - \varepsilon(0)] = \int_{0}^{t} \tau(\gamma) \frac{d}{d\gamma} e(\gamma)\, d\gamma \tag{3.9}$$

Consider this result for the case of a simple harmonic stress field

$$\tau(t) = \mathrm{Re}\{-i\ e^{i\omega t}\tau_{max}\} = \tau_{max}\, sin(\omega t) \tag{3.10}$$

where τ_{max} is a scalar constant giving the maximum stress. For the associated strain the correspondence principle gives

$$e(t) = \mathrm{Re}\{\frac{\tau(t)}{\tilde{C}(\omega)}\} \tag{3.11}$$

In the course of a single cycle the elastic strain energy will increase and then decrease. It can be shown that the maximum strain energy is reached when

$$\omega t = \frac{3\pi}{2} + \theta_C \tag{3.12}$$

and the maximum value is

$$max[\rho\varepsilon] = \frac{\tau_{max}^2}{2}\mathrm{Re}\{\tilde{C}(\omega)\}(1 + (\frac{3\pi}{2}+\theta_C)tan(\theta_C)) \tag{3.13}$$

At the end of a single cycle ($t = 2\pi/\omega$) there will be a net loss of energy given by

$$\Delta[\rho\varepsilon] = \pi\,\tau_{max}^2\,\mathrm{Im}\{\tilde{C}(\omega)\} \tag{3.14}$$

A quantity of interest is the ratio of the energy loss per radian to the maximum energy, which is often used to define a quality factor directly related to energy.

$$Q_\varepsilon^{-1} \equiv \frac{\Delta[\rho\varepsilon]}{2\pi\ max[\rho\varepsilon]} \tag{3.15}$$

Using the results derived above, this becomes

$$Q_\varepsilon^{-1} = \frac{\mathrm{Im}\{\tilde{C}(\omega)\}}{\mathrm{Re}\{\tilde{C}(\omega)\}(1 + (\frac{3\pi}{2}+\theta_C)\tan(\theta_C))} \tag{3.16}$$

If the viscous effects are small compared to the elastic effects, then $Q^{-1} \ll 1$ and

$$Q_\varepsilon^{-1} = Q^{-1} \tag{3.17}$$

and the difference in the two definitions of Q is not important. However, when viscous effects are appreciable the difference between the two definitions must be taken into account, and the exact relationship is

$$Q_\varepsilon^{-1} = \frac{Q^{-1}}{1 + (\frac{3\pi}{2}+\tan^{-1}(Q^{-1}))Q^{-1}} \tag{3.18}$$

In experimental work it is common to define the *damping ratio* as

$$d \equiv \frac{\Delta[\rho\varepsilon]}{2\pi\ \max[\tau(t)]\ \max[e(t)]} \tag{3.19}$$

and this leads to

$$d = \frac{1}{2}\sin(\theta_C) \tag{3.20}$$

In terms of the seismic definition of Q^{-1}, the relationship for the damping ratio is

$$Q^{-1} = \frac{2d}{\sqrt{1-4d^2}} \tag{3.21}$$

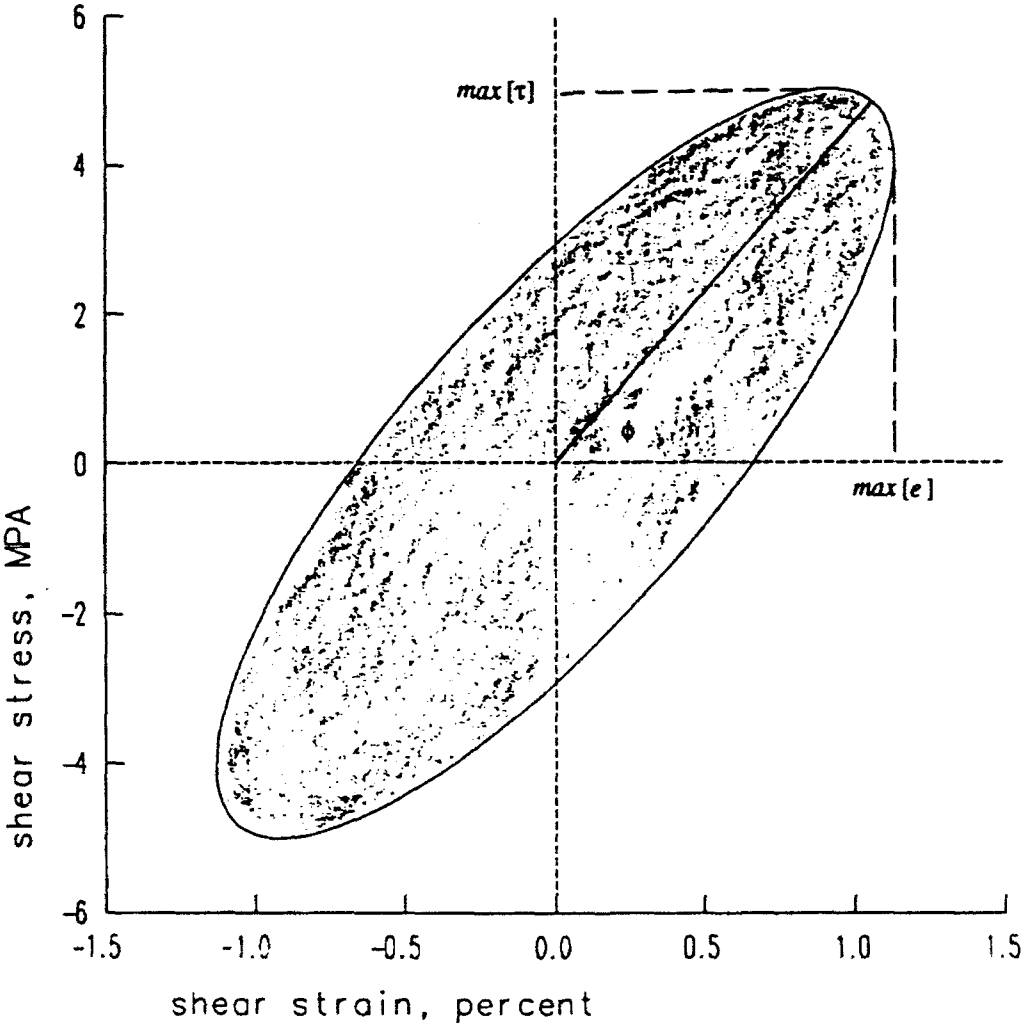

Figure 1. A hysteresis curve and the parameters which can be used to describe it. The area of the ellipse is a measure of $\Delta[\rho\varepsilon]$ and the slope of a line through the end points of the curve is $S_h = \tan(\phi)$. The maximum values of stress and strain are also shown.

A convenient method of analyzing the energy relationships of visco-elastic materials is in terms of hysteresis curves. A cyclic loading of the material results in a stress-strain curve such as that shown in Figure 1. For a linear visco-elastic material this curve is an ellipse. The area enclosed by the curve is a measure of the energy loss per cycle $\Delta[\rho\varepsilon]$ and the maximum stress and maximum strain are also easily measured from the curve, so equation (3.19) can be used to estimate the damping ratio of the material. Then equation (3.21) leads to an estimate of the seismic quality factor.

The slope of a straight line through the end points of the hysteresis curve can be used to provide an estimate of the modulus of the elastic constant $|\hat{C}(\omega)|$. If S_h is the slope of this line, then it can be shown that

$$|\hat{C}(\omega)| = \frac{[(S_h^2+1)^2-4S_h^2Q^{-2}]^{1/2} + S_h^2-1}{2S_h[1+Q^{-2}]^{1/2}} \tag{3.22}$$

Figure 1 illustrates how an estimate of the elastic modulus can be obtained from a hysteresis curve. The four quantities $\max[e]$, $\max[\tau]$, ϕ, and $\Delta[\rho\varepsilon]$ can be measured directly from the curve. Then equation 3.22 yields an estimate of the absolute value of the elastic modulus and equations 3.19, 3.21, and 3.8 yield an estimate of its phase. Hence, the complete complex elastic modulus can be obtained from the hysteresis curve. This estimate of the elastic modulus will in general be a function of the level of stress and strain.

Hysteresis curves such as shown in Figure 1 provide a convenient method for the experimental determination of the elastic properties of earth materials. Both stress and strain are measured as a cyclic stress is applied and the result is a direct determination of the hysteresis curve. In general the resulting curve for actual earth materials will not be an ellipse, but the quantities $\max[e]$, $\max[\tau]$, ϕ, and $\Delta[\rho\varepsilon]$ can still be extracted from the curve and converted to an equivalent linear elastic modulus (see for example Idriss and Seed (1968) and Hardin and Drnevich (1972a)).

Figure 2 shows hysteresis loops that were calculated for three different stress levels in a material having the properties of wet tuff. These properties were taken to be $\rho_u = 2.58\ gm/cm^3$, $e_r = 10^{-4}$, and $d_{max} = 0.30$. The equivalent elastic treatment of section 2 was used to adjust the material properties as the peak stress and strain were changed. In the case of compressional stress, there is a slight increase in the real part of the modulus as the stress increases and the imaginary part also increases. In the case of shear stress, there is a marked decrease in the real part of the modulus and an increase in the imaginary part as the level of the stress increases. The numerical values corresponding to these hysteresis curves are listed in Table 1. In this table case 0 is the low stress situation, and cases 1 through 3 are the situations shown in Figure 2 as the stress level is increased.

Table 1. Equivalent elastic constants for the hysteresis curves of Figure 2.

	Case 0	Case 1	Case 2	Case 3
Peak pressure (MPA)	0	5	10	30
Peak shear stress (MPA)	0	1	3	10
Density (gm/cc)	2.10	2.10	2.10	2.11
P velocity (km/sec)	2.85	2.85	2.85	2.86
S velocity (km/sec)	1.45	0.94	0.69	0.41
Q_p^{-1}	0.01	0.18	0.23	0.26
Q_s^{-1}	0.02	0.48	0.63	0.72

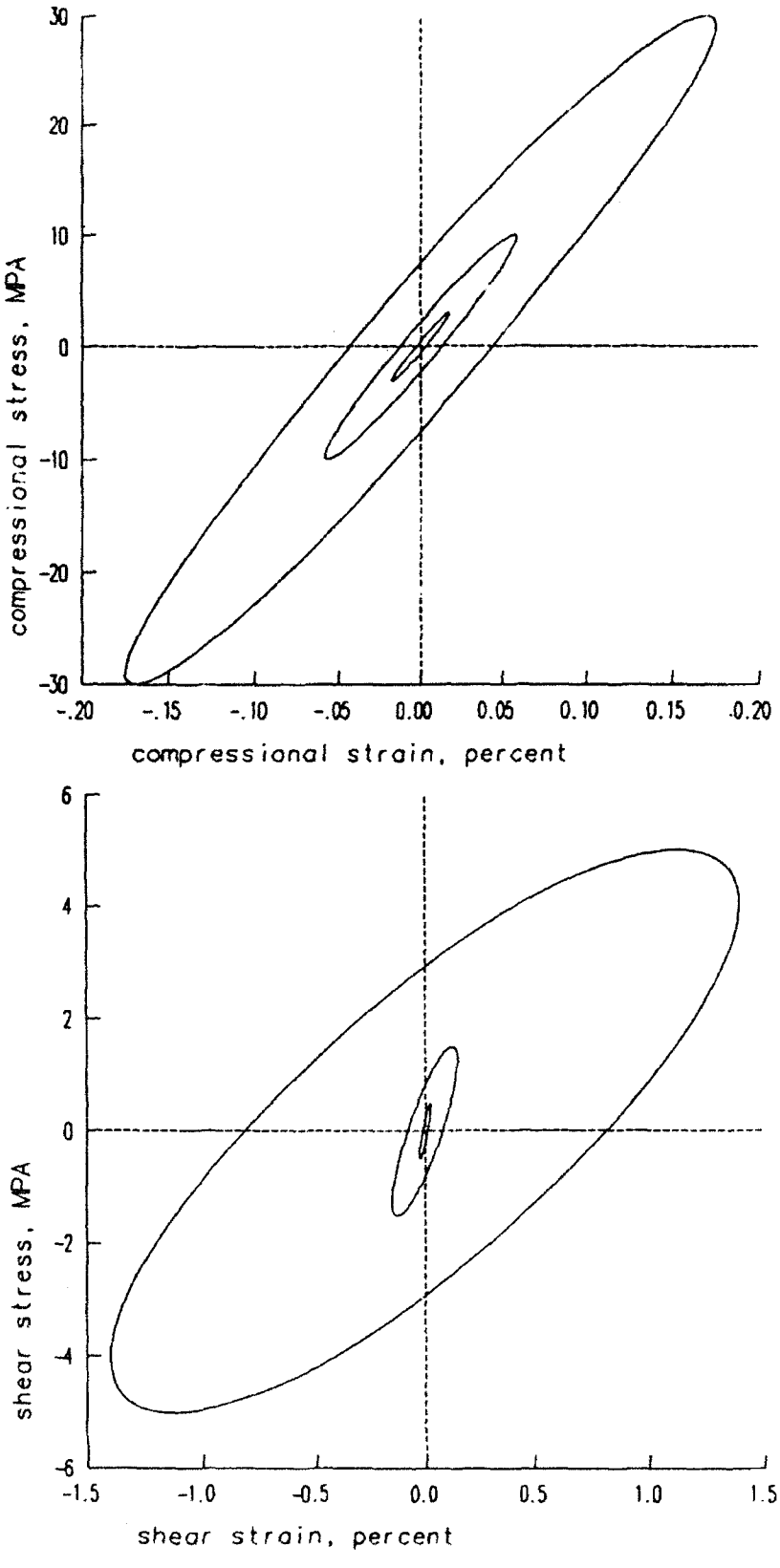

Figure 2. Hysteresis curves for both compression and shear at three different levels of strain in wet tuff. The equivalent elastic treatment was used for both the real and imaginary parts of the elastic moduli.

4. Elastic Wave Propagator Solution

The use of the equivalent elastic method requires that the elastodynamic equations of motion be solved for an explosive source in an inhomogeneous medium. Standard propagator methods can be used to solve this problem.

Consider an explosive source centered at the origin and assume complete spherical symmetry so that all displacements will be in the radial direction and only compressional waves will be generated. Adopting a spherical coordinate system and assuming a harmonic time dependence of the form $e^{i\omega t}$, the displacement can be written as

$$\mathbf{u} = u(r,\omega)\,\hat{\mathbf{r}} \tag{4.1}$$

where $\hat{\mathbf{r}}$ is the unit vector in the radial direction. In a region where the equations of linear elasticity are obeyed the displacement must satisfy

$$(\lambda+2\mu)\nabla^2\mathbf{u} - \nabla\times\nabla\mathbf{u} + \rho\omega^2\mathbf{u} = 0 \tag{4.2}$$

where ρ is the density and λ , μ are the Lame elastic constants. In a region where these elastic parameters are independent of the spatial coordinates, a general solution to the above equation is

$$\mathbf{u}(r,\omega) = a^{(1)}h_1^{(1)}(k_p r)\hat{\mathbf{r}} + a^{(2)}h_1^{(2)}(k_p r)\hat{\mathbf{r}} \tag{4.3}$$

Here $h_l^{(1)}$ and $h_l^{(2)}$ are spherical Hankel functions of the first and second kind, respectively, and

$$k_p \equiv \frac{\omega}{V_p} \tag{4.4}$$

where

$$V_p \equiv \left[\frac{\lambda+2\mu}{\rho}\right]^{1/2} \tag{4.5}$$

It is easily demonstrated that the function $h_l^{(1)}$ represents inward traveling compressional waves, while $h_l^{(2)}$ represents outward traveling waves. The terms $a^{(1)}$ and $a^{(2)}$ are arbitrary constants at this point.

The radial traction on any surface of constant radius has the form

$$\mathbf{t}_r = \lambda\nabla\cdot\mathbf{u}\hat{\mathbf{r}} + 2\mu\frac{\partial}{\partial r}\mathbf{u} + \mu\hat{\mathbf{r}}\times\nabla\times\mathbf{u} = \tau_{rr}(r,\omega)\hat{\mathbf{r}} \tag{4.6}$$

Corresponding to the solution for $\mathbf{u}$ given above, this stress is

$$\tau_{rr}(r,\omega) = a^{(1)}\left[(\lambda+2\mu)k_p h_0^{(1)}(k_p r) - \frac{4\mu}{r}h_1^{(1)}(k_p r)\right] + a^{(2)}\left[(\lambda+2\mu)k_p h_0^{(2)}(k_p r) - \frac{4\mu}{r}h_1^{(2)}(k_p r)\right] \tag{4.7}$$

The tangential stresses are

$$\tau_{\theta\theta}(r,\omega) = \tau_{\phi\phi}(r,\omega) = a^{(1)}\left[\lambda k_p h_0^{(1)}(k_p r) + \frac{2\mu}{r} h_1^{(1)}(k_p r)\right]$$

$$+ a^{(2)}\left[\lambda k_p h_0^{(2)}(k_p r) + \frac{2\mu}{r} h_1^{(2)}(k_p r)\right] \tag{4.8}$$

Now consider the region around the source to be divided into a number of spherical shells, with the material properties constant within each shell but possibly changing at the boundaries between shells. Shell n will be bounded by radii r_n and r_{n+1} and will have material properties ρ_n, λ_n, μ_n. We also have $k_n = \omega/V_{pn}$. Using the results developed above, the displacement and radial stress within the n-th shell can be written in matrix form as

$$\begin{bmatrix} u \\ t_r \end{bmatrix} = \mathbf{A}_n \begin{bmatrix} a_n^{(1)} \\ a_n^{(2)} \end{bmatrix} \tag{4.9}$$

where the shell matrix $\mathbf{A}$ is defined as

$$\mathbf{A}_n(r,\omega) \equiv \begin{bmatrix} h_1^{(1)}(k_n r) & h_1^{(2)}(k_n r) \\ [(\lambda_n+2\mu_n)k_n h_0^{(1)}(k_n r) - \frac{4\mu_n}{r} h_1^{(1)}(k_n r)] & [(\lambda_n+2\mu_n)k_n h_0^{(2)}(k_n r) - \frac{4\mu_n}{r} h_1^{(2)}(k_n r)] \end{bmatrix} \tag{4.10}$$

It is easily shown that the inverse of this matrix exists and is given by

$$\mathbf{A}_n^{-1}(r,\omega) = \frac{ik_n r^2}{2(\lambda_n+2\mu_n)} \begin{bmatrix} [(\lambda_n+2\mu_n)k_n h_0^{(2)}(k_n r) - \frac{4\mu_n}{r} h_1^{(2)}(k_n r)] & -h_1^{(2)}(k_n r) \\ -[(\lambda_n+2\mu_n)k_n h_0^{(1)}(k_n r) - \frac{4\mu_n}{r} h_1^{(1)}(k_n r)] & h_1^{(1)}(k_n r) \end{bmatrix} \tag{4.11}$$

The boundary conditions for this problem are that u and t_r should be everywhere continuous. This means that at the radius r_n where shells n and n-1 are in contact the following equation must hold.

$$\begin{bmatrix} u \\ t_r \end{bmatrix} = \mathbf{A}_{n-1}(r_n,\omega) \begin{bmatrix} a_{n-1}^{(1)} \\ a_{n-1}^{(2)} \end{bmatrix} = \mathbf{A}_n(r_n,\omega) \begin{bmatrix} a_n^{(1)} \\ a_n^{(2)} \end{bmatrix} \tag{4.12}$$

It follows that

$$\begin{bmatrix} a_n^{(1)} \\ a_n^{(2)} \end{bmatrix} = \mathbf{A}_n^{-1}(r_n,\omega)\ \mathbf{A}_{n-1}(r_n,\omega) \begin{bmatrix} a_{n-1}^{(1)} \\ a_{n-1}^{(2)} \end{bmatrix} \tag{4.13}$$

It is convenient to define an interface matrix as

$$\mathbf{B}_n(\omega) \equiv \mathbf{A}_n^{-1}(r_n,\omega)\ \mathbf{A}_{n-1}(r_n,\omega) \tag{4.14}$$

Letting $z_n = k_n r_n$ and $z_{n-1} = k_{n-1} r_n$, the individual elements of $\mathbf{B}_n$ are

$$B_{11} = \frac{z_n e^{-i(z_n - z_{n-1})}}{2(\lambda_n + 2\mu_n)} \left[(\lambda_n + 2\mu_n) \frac{i + z_{n-1}}{z_{n-1}^2} - (\lambda_{n-1} + 2\mu_{n-1}) \frac{i - z_n}{z_n^2} + 4i(\mu_n - \mu_{n-1}) \frac{(i - z_n)(i + z_{n-1})}{z_n^2 z_{n-1}^2} \right] \quad (4.15a)$$

$$B_{12} = \frac{-z_n e^{-i(z_n + z_{n-1})}}{2(\lambda_n + 2\mu_n)} \left[(\lambda_n + 2\mu_n) \frac{i - z_{n-1}}{z_{n-1}^2} - (\lambda_{n-1} + 2\mu_{n-1}) \frac{i - z_n}{z_n^2} + 4i(\mu_n - \mu_{n-1}) \frac{(i - z_n)(i - z_{n-1})}{z_n^2 z_{n-1}^2} \right] \quad (4.15b)$$

$$B_{21} = \frac{z_n e^{i(z_n + z_{n-1})}}{2(\lambda_n + 2\mu_n)} \left[(\lambda_n + 2\mu_n) \frac{i + z_{n-1}}{z_{n-1}^2} - (\lambda_{n-1} + 2\mu_{n-1}) \frac{i + z_n}{z_n^2} + 4i(\mu_n - \mu_{n-1}) \frac{(i + z_n)(i + z_{n-1})}{z_n^2 z_{n-1}^2} \right] \quad (4.15c)$$

$$B_{22} = \frac{-z_n e^{i(z_n - z_{n-1})}}{2(\lambda_n + 2\mu_n)} \left[(\lambda_n + 2\mu_n) \frac{i - z_{n-1}}{z_{n-1}^2} - (\lambda_{n-1} + 2\mu_{n-1}) \frac{i + z_n}{z_n^2} + 4i(\mu_n - \mu_{n-1}) \frac{(i + z_n)(i - z_{n-1})}{z_n^2 z_{n-1}^2} \right] \quad (4.15d)$$

This process of matching boundary conditions at an interface can be repeated at successive boundaries, and thus the solution can be propagated through an arbitrary number of shells. Assuming the process to have started in shell 1, the solution in shell n is

$$\begin{bmatrix} a_n^{(1)} \\ a_n^{(2)} \end{bmatrix} = \mathbf{B}_n(\omega)\, \mathbf{B}_{n-1}(\omega) \quad \cdots \quad \mathbf{B}_2(\omega) \begin{bmatrix} a_1^{(1)} \\ a_1^{(2)} \end{bmatrix} \quad (4.16)$$

The next step is to assume that shell 0 consists of a gas having pressure P and adiabatic gas constant γ. Then, allowing approximately for the change in pressure caused by the expansion of the shell, the displacement-stress vector at the radius r_1 will be

$$\begin{bmatrix} u \\ t_r \end{bmatrix} = \begin{bmatrix} u \\ -P(1 - 3\gamma u / r_1) \end{bmatrix} = \mathbf{A}_1(r_1, \omega) \begin{bmatrix} a_1^{(1)} \\ a_1^{(2)} \end{bmatrix} \quad (4.17)$$

Two independent trial solutions can be obtained for this system. First assume that $a_1^{(2)} = 0$ and then it is possible to solve for

$$a_1^{(1)} = \frac{-P}{(\lambda_1 + 2\mu_1) k_1 h_0^{(1)}(k_1 r_1) - \frac{4}{r_1}(\mu_1 + \frac{3\gamma P}{4}) h_1^{(1)}(k_1 r_1)} \quad (4.18a)$$

The second solution is obtained by assuming that $a_1^{(1)} = 0$ and then

$$a_1^{(2)} = \frac{-P}{(\lambda_1 + 2\mu_1) k_1 h_0^{(2)}(k_1 r_1) - \frac{4}{r_1}(\mu_1 + \frac{3\gamma P}{4}) h_1^{(2)}(k_1 r_1)} \quad (4.18b)$$

The general solution is obtained by introducing the parameter ε, and then the sum of ε times the first trial solution and $(1-\varepsilon)$ times the second trial solution will satisfy the boundary conditions at r_1.

The parameter ε is determined by the radiation condition. Assume that shell N extends to infinity so that there are only outward propagating waves in this region, and thus $a_N^{(1)} = 0$. This means that

$$\varepsilon\, a_{N1}^{(1)} + (1-\varepsilon)\, a_{N2}^{(1)} = 0 \tag{4.19}$$

where a_{N1} and a_{N2} are the two solutions that are obtained in shell N when the two different trial solutions from r_1 are propagated independently to r_N. It follows that

$$\varepsilon = \frac{a_{N2}^{(1)}}{a_{N2}^{(1)} - a_{N1}^{(1)}} \tag{4.20}$$

Having determined ε, the two trial solutions can be summed with the proper weighting factors at any radius to yield the total solution.

The case of an explosion in a medium where a hydrostatic pressure is present is obtained from the above solution by letting the pressure on the cavity wall be $P - P_l$, where P_l is the lithostatic pressure at the shot point. Then all of the pressures and stresses that are calculated will be departures from the initial hydrostatic case. With this approach the initial stress $\boldsymbol{\tau}_o = -P_l \mathbf{I}$ is homogeneous so $\nabla \cdot \boldsymbol{\tau}_o = 0$ and there is no change is the basic equations. However, if the initial pressure is not homogeneous, such as when the depth effect of pressure is included, the solution loses its spherical symmetry and becomes more complicated.

The possibility that elastic waves will be attenuated as they propagate is included by introducing anelasticity into the problem. This is achieved by using the correspondence principle to generalize the previous results. This consists of introducing the complex elastic constants

$$\lambda + 2\mu \rightarrow (\lambda + 2\mu)(1 + iQ_p^{-1}) \tag{4.21a}$$

and

$$\mu \rightarrow \mu(1 + iQ_s^{-1}) \tag{4.21b}$$

The wave number k_p will now be complex also and can be written

$$k_p \rightarrow k_p(1 - i\delta) \tag{4.22}$$

The requirement that the elastodynamic equations be satisfied leads to

$$k_p = \omega\left[\frac{\rho}{\lambda+2\mu}\,\frac{1}{1+Q_p^{-2}}\,\frac{1+[1+Q_p^{-2}]^{1/2}}{2}\right]^{1/2} \tag{4.23a}$$

and

$$\delta = \frac{1}{Q_p\,(1+[1+Q_p^{-2}]^{1/2})} \tag{4.23b}$$

A similar set of equations can be derived for the wavenumber k_s. Note that in general Q_p and Q_s will be functions of frequency.

With attenuation present, the velocities will in general be dispersive. Assuming that Q_p and Q_s are not functions of frequency in the band of interest, causality is maintained by requiring that

$$V_p(f) = V_p(f_r)\left[1 + \frac{1}{\pi Q_p}\ln[\frac{f}{f_r}]\right] \tag{4.24a}$$

$$V_s(f) = V_s(f_r)\left[1 + \frac{1}{\pi Q_s}\ln[\frac{f}{f_r}]\right] \tag{4.24b}$$

where f_r is some reference frequency.

5. Method of Calculation

The basic steps of the computational scheme are outlined in Figure 3. The first step is to initialize the model of the material properties surrounding the explosion. This consists of dividing the region into an appropriate number of spherical shells and specifying the initial material properties for these shells. The material properties are assumed to be constant within each shell. The parameters associated with the equivalent elastic treatment, such as the ultimate density, the reference shear strain, and the maximum damping must also be specified at this time. The outside radius of the last shell should be large enough so that the material properties at this and greater distances can be safely assumed to be linear visco-elastic.

The second step is to initialize the properties of the explosive source. The size of the explosion is specified by giving its chemical energy E_o. The initial radius of the cavity r_o is also specified, which leads to the initial volume

$$V_o = \frac{4}{3}\pi r_o^3 \tag{5.1}$$

The explosion is assumed to take place instantaneously so that at $t = 0$ the initial pressure within the cavity increases by an amount

$$P_o = \frac{E_o(\gamma-1)}{V_o} \tag{5.2}$$

where γ is the gas constant for the explosive gasses. This initial pressure is the radial stress at $r = r_o$, which is one of the boundary conditions for the elastic wave solution.

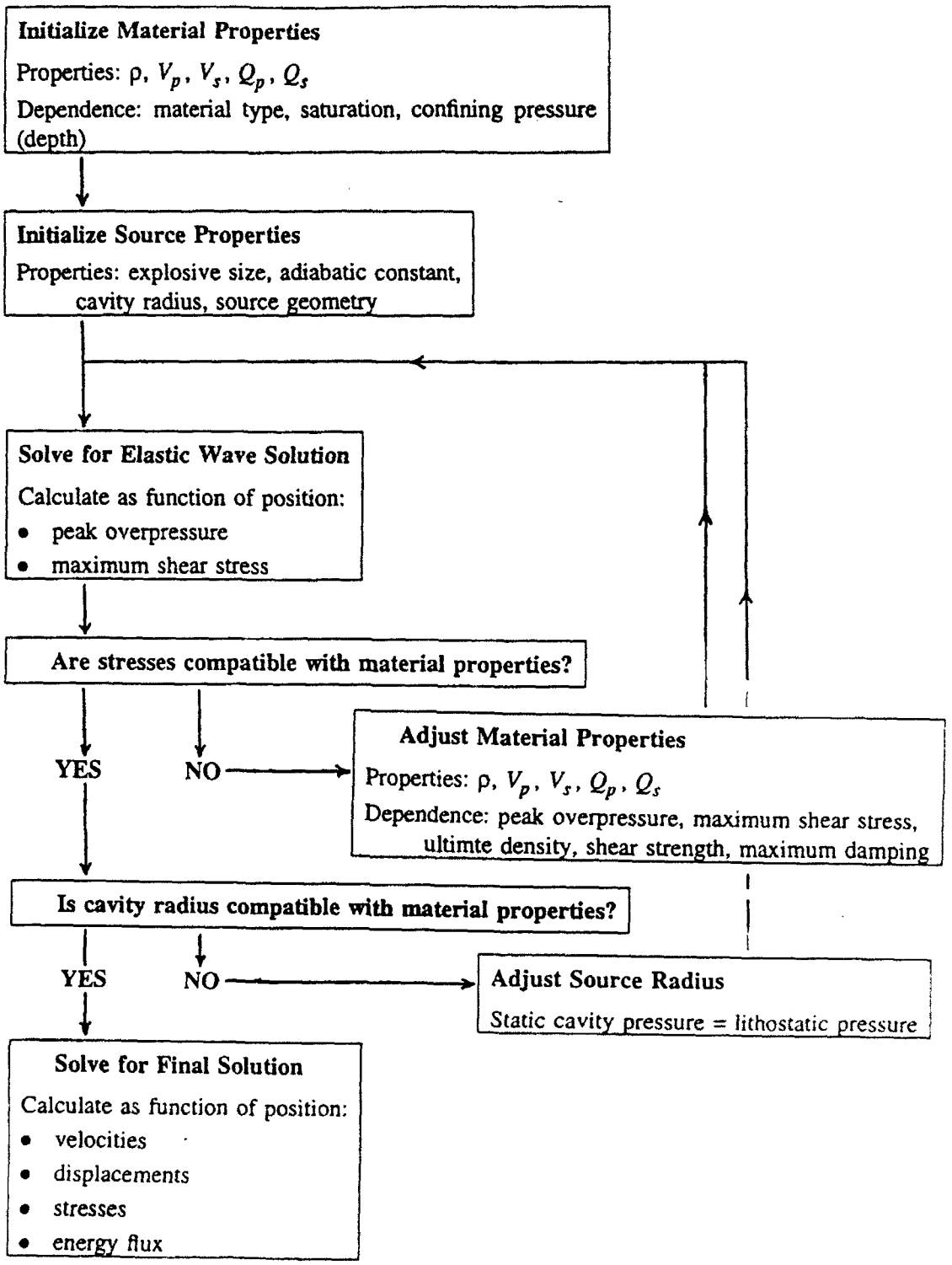

Figure 3. Flow chart for the calculation of the outward propagating waves from an explosive source using the equivalent elastic method.

The third step is to obtain the elastic wave solution for the entire region surrounding the source using the propagator solutions of section 4. Given this solution, the stresses and strains at all distances from the source can be calculated. In general the stresses associated with this solution will be sufficiently large so that the initial material properties are not appropriate. Thus the material properties are adjusted on the basis of the calculated stresses and the equivalent elastic treatment outlined in section 2. For the purposes of this adjustment the pressure is

$$P = -\frac{\tau_{rr} + \tau_{\theta\theta} + \tau_{\phi\phi}}{3} \tag{5.3}$$

and the shear stress is

$$\tau = \frac{\tau_{\theta\theta} - \tau_{rr}}{2} \tag{5.4}$$

Having adjusted the material properties in all of the shells, the elastic wave solution can be obtained for the adjusted model and the entire process repeated. This iterative process of solving for the stresses and adjusting the material properties is repeated until a solution is obtained in which the stresses are compatible with the material properties at all distances. Generally, only three or four iterations are required.

After convergence of the process of adjusting the material properties, the source radius is also adjusted to allow for the inelastic growth of the cavity. The cavity radius r_a is increased by successively eliminating shells until the static pressure is less than some factor times the lithostatic pressure

$$P(r_a, t \rightarrow \infty) \leq \eta P_l \tag{5.5}$$

Here the lithostatic pressure P_l is just that due to the overburden and is given by

$$P_l = \rho_o g z_s \tag{5.6}$$

where g is the acceleration of gravity and z_s is the source depth. Recall that the calculated pressure is in excess of the lithostatic pressure, so this condition actually corresponds to the static cavity pressure being $1+\eta$ times the lithostatic pressure. For the calculations in tuff the factor η was assumed to have a value of 0.5.

After the adjustment of the cavity radius, a final iteration is performed on the adjustment of the material properties to insure that the stresses and material properties at all distances from the source are compatible. At the completion of this step the final solution is available.

6. Experimental Check of the Method

This method of calculating fields of an explosive source is illustrated by some initial calculations in Figure 4. The upper panel shows the first 10 msec of measured particle velocity within a few meters of a buried chemical explosion, while the lower panel shows the results of simulating these measurements with the code that employs equivalent elastic material properties. The data were obtained during the OSSY2 experiments of 1991.

The OSSY2 (On Site Seismic Yield) experiments were performed in 1991 in Yucca Valley at the Nevada Test Site. They were a cooperative effort between scientists at Lawrence Livermore National Laboratory, Lawrence Berkeley Laboratory, the Seismographic Station at UC Berkeley, and Southern Methodist University. The data shown in Figure 4 were obtained from a chemical explosion that was detonated at a depth of 534 meters in hole UE4av. The source size was 100 pounds of C4 explosive. The source medium was a bedded tuff immediately above the Grouse Canyon member. The source properties which were used in the calculation are

$$\rho_o = 2.10\ gm/cm^3 \quad , \quad V_{po} = 2.85\ km/sec \quad , \quad V_{so} = 1.45\ km/sec$$

As mentioned in section 2, the equivalent elastic parameters used in the calculations were $\rho_u = 2.58 gm/cm^3$, $e_r = 10^{-4}$, and $d\max = 0.30$. These estimates of material properties were based on the results of a VSP survey (Leonard et al, 1992) and laboratory measurements (Emerick, 1966).

Starting with the material properties listed above as initial values, the elastic wave solutions were obtained out to a distance of 40 meters from the source point. Using the stresses that resulted from this solution, the material properties were adjusted according to the method described in section 2. Then a new wave solution was obtained using the modified material properties. This process was repeated until there was essentially no change in material properties between iterations.

The equivalent elastic modification of the material properties was most pronounced in a region that extended out to about 2 meters from the shot point. In this region the density and compressional velocity were increased by up to 5% while the shear velocity and shear quality factor were decreased by over 90%. At larger distances there was little modification in the density and compressional velocity, although there were significant but decreasing effects upon the shear velocity and shear quality factor out to distances of about 10 meters.

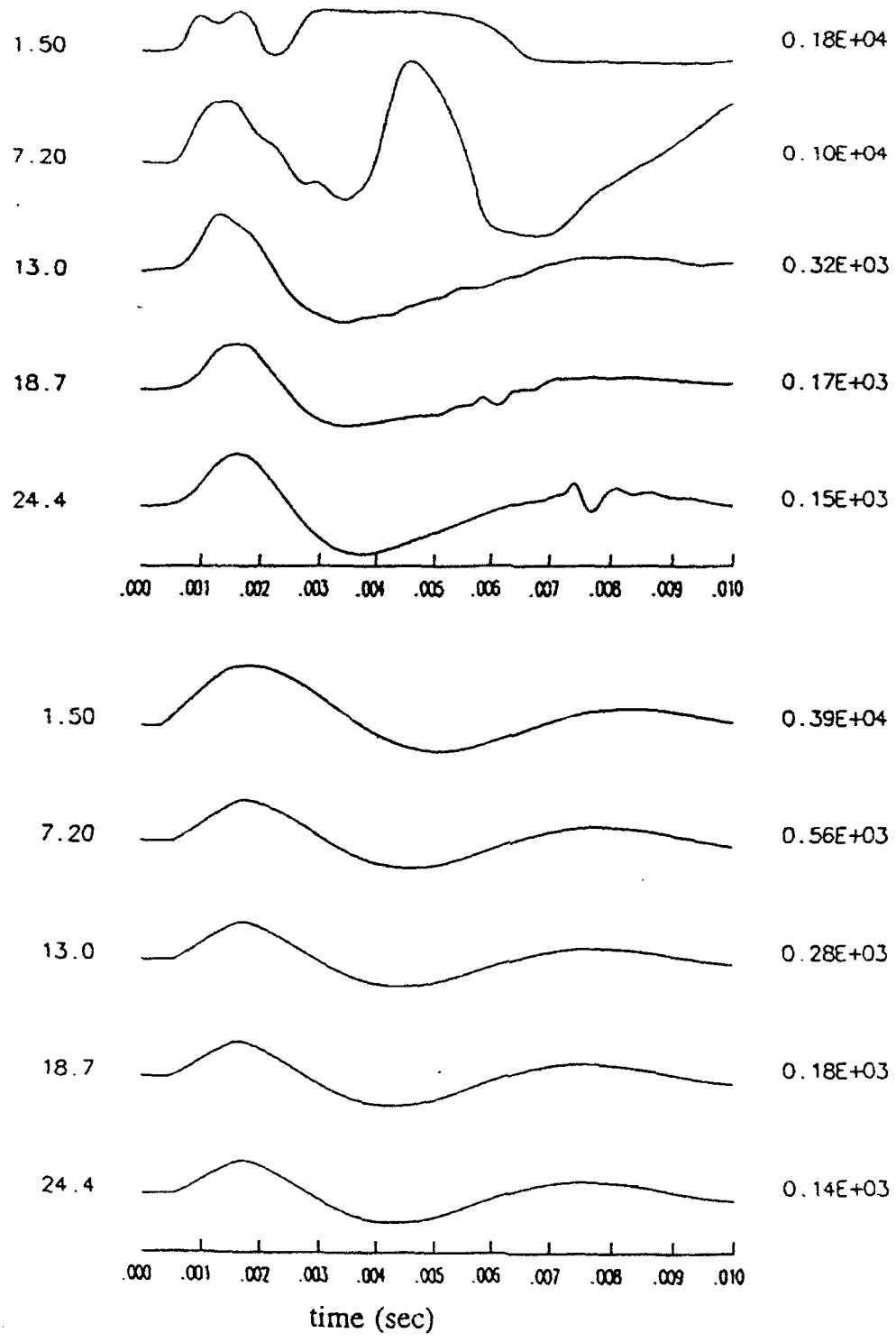

Figure 4. Recorded and calculated free field measurements of velocities from a chemical explosion. The explosion consisted of 100 pounds of C4 explosive which was detonated at a depth of 534 meters in Yucca Valley. The upper panel shows velocities that were recorded by a linear array of instruments directly above the explosion. The number on the left of each trace is the radial distance of the instrument from the center of the explosion in meters and the number on the right is the maximum velocity in cm/sec. The traces have been multiplied by distance from the explosion for the purposes of plotting.

The next step was to calculate a new effective cavity radius for the source. The criterion used was that the static cavity pressure should equal 1.5 times the lithostatic pressure. This resulted in the cavity radius increasing from 9 cm to 20 cm. Another iteration of the equivalent elastic adjustment of material properties was then performed, with the main result being a further reduction in the shear velocity in the immediate vicinity of the new cavity radius. Finally, using the effective material properties and the effective cavity radius, a final wave solution was obtained to yield the results shown in the lower panel of Figure 4.

The agreement between the observed and calculated velocities in Figure 4 indicates some promise for this type of an approach. The recordings at the two closest distances of 1.5 and 7.2 meters are somewhat suspect, so the comparison here may not be valid. The acceleration at the first gage was in excess of 8000 g and there is a suggestion on the acceleration record that the gage may have broken loose and gone into ballistic motion. The acceleration at the second gage was greater than 2500 g and the maximum acceleration occurs during the second pulse that is delayed by about 3 msec, which is difficult to explain in terms of an outgoing pressure wave. Note that both of these gages were in the range of strongly nonlinear material behavior in the sense that the equivalent elastic treatment resulted in significant modifications. At the three outer gages the observed records seem more reasonable, indicating an outward propagating wave that changes slowly with distance. The simulated records agree quite well in amplitude and period in this range, although the asymmetry in the waveforms in somewhat different for the observed and calculated results. One possible explanation for this difference is that the dispersion associated with the anelastic properties of the medium has not been properly modeled in the simulations. This, along with many other aspects of the simulation calculations, need considerably more investigation.

7. Conclusions

The approach described here is not a substitute for complete equation-of-state codes, but it appears to provide an effective method of investigating some of the basic elements of wave propagation near an explosive source. The computer codes are quite efficient, so that it is possible to perform extensive simulation studies in which the role of various parameters is investigated. Thus the method is quite useful in helping to isolate the model parameters which are controlling some particular feature of the observational data.

Considerable more testing must be performed in order to establish that this method produces reliable quantitative estimates of the seismic waveforms which are transmitted to the linear elastic region.

So far most of the comparisons with observational data have involved chemical explosions, because such data were conveniently available, but such comparisons must be extended to nuclear explosions. It would also be helpful to extend the comparisons to other types of source media.

One characteristic of the equivalent elastic method is that it requires a relationship between material properties and the level of strain. Further development and use of this method will require the assembly of a data base of empirical relationships for equivalent elastic treatments that covers all of the different types of materials which might serve as source media for explosions. The literature contains considerable data of this type for various soils, but comparable data pertaining to hard rocks has not yet been located. However, a complete search of the literature with respect to this type of information has not been completed.

While the feasibility of the method investigated in this study has not yet been firmly established, the exercise has been successful in demonstrating the need for approaches of this type which produce simple analytic results. One of the advantages of such an approach is that it allows various features of the observational data to be explored with respect to their cause and uniqueness. The relative role of the material inside and outside the elastic radius in determining the frequency content of the radiated seismic energy is one such area of interest. Another is the relationship between the corner frequency of the spectrum and the source radius. For instance, the initial calculations suggest that the effective source radius may be a rather vaguely defined quantity. It is also possible to explore the role of the energy density within the cavity, which relates to the differences between chemical and nuclear explosions and methods of decoupling explosions in an enlarged cavity.

8. References

Aki, K., and P. G. Richards, Quantitative Seismology, Vol. I, W. H. Freeman, San Francisco, 557 pp, 1980.

Denny, M. D., and L. R. Johnson, The explosion seismic source function: models and scaling laws revisited, p. 1-24 in Explosion Source Phenomenology, edited by S. R. Taylor, H. J. Patton, and P. G. Richards, Geophys. Monograph 65, American Geophysical Union, Washington, D.C., 1991.

Emerick, W. L., Physical properties of volcanic rocks, Rainier Mesa and vicinity, Nevada Test Site, U.S. Geol. Surv., Technical Letter: Area 12-18, 21 pp, 1966.

Hardin, B. O., and V. P. Drnevich, Shear modulus and damping in soils: measurement and parametric effects, J. Soil Mech. and Found. Div., Proc. Am. Soc. Civil Eng., 98, 603-624, 1972a.

Hardin, B. O., and V. P. Drnevich, Shear modulus and damping in soils: design equations and curves, J. Soil Mech. and Found. Div., Proc. Am. Soc. Civil Eng., 98, 667-692, 1972b.

Idriss, I. M., and H. B. Seed, Seismic response of horizontal soil layers, J. Soil Mech. and Found. Div., Proc. Am. Soc. Civil Eng., 94, 1003-1031, 1968.

Latter, A. L., E. A. Martinelli, and E. Teller, Seismic scaling law for underground explosions, Phys. of Fluids, 2, 280-282, 1959.

Leonard, M. A., T. M. Daley, L. R. Johnson, and T. V. McEvilly, VSP site characterization at NTS: OSSY91 - Summary report, LBL Topical Report LBL-32521, April, 1992.

Majtenyi, S. I., and E. L. Foster, Propagation velocity of shock waves and presure waves in soil and rock, Geophys. Res. Let., 19, 865-868, 1992.

Prof. Thomas Ahrens
Seismological Lab, 252-21
Division of Geological & Planetary Sciences
California Institute of Technology
Pasadena, CA 91125

Prof. Keiiti Aki
Center for Earth Sciences
University of Southern California
University Park
Los Angeles, CA 90089-0741

Prof. Shelton Alexander
Geosciences Department
403 Deike Building
The Pennsylvania State University
University Park, PA 16802

Prof. Charles B. Archambeau
CIRES
University of Colorado
Boulder, CO 80309

Dr. Thomas C. Bache, Jr.
Science Applications Int'l Corp.
10260 Campus Point Drive
San Diego, CA 92121 (2 copies)

Prof. Muawia Barazangi
Institute for the Study of the Continent
Cornell University
Ithaca, NY 14853

Dr. Jeff Barker
Department of Geological Sciences
State University of New York
at Binghamton
Vestal, NY 13901

Dr. Douglas R. Baumgardt
ENSCO, Inc
5400 Port Royal Road
Springfield, VA 22151-2388

Dr. Susan Beck
Department of Geosciences
Building #77
University of Arizona
Tuscon, AZ 85721

Dr. T.J. Bennett
S-CUBED
A Division of Maxwell Laboratories
11800 Sunrise Valley Drive, Suite 1212
Reston, VA 22091

Dr. Robert Blandford
AFTAC/TT, Center for Seismic Studies
1300 North 17th Street
Suite 1450
Arlington, VA 22209-2308

Dr. Stephen Bratt
ARPA/NMRO
3701 North Fairfax Drive
Arlington, VA 22203-1714

Dr. Lawrence Burdick
IGPP, A-025
Scripps Institute of Oceanography
University of California, San Diego
La Jolla, CA 92093

Dr. Robert Burridge
Schlumberger-Doll Research Center
Old Quarry Road
Ridgefield, CT 06877

Dr. Jerry Carter
Center for Seismic Studies
1300 North 17th Street
Suite 1450
Arlington, VA 22209-2308

Dr. Eric Chael
Division 9241
Sandia Laboratory
Albuquerque, NM 87185

Dr. Martin Chapman
Department of Geological Sciences
Virginia Polytechnical Institute
21044 Derring Hall
Blacksburg, VA 24061

Prof. Vernon F. Cormier
Department of Geology & Geophysics
U-45, Room 207
University of Connecticut
Storrs, CT 06268

Prof. Steven Day
Department of Geological Sciences
San Diego State University
San Diego, CA 92182

Marvin Denny
U.S. Department of Energy
Office of Arms Control
Washington, DC 20585

Dr. Zoltan Der
ENSCO, Inc.
5400 Port Royal Road
Springfield, VA 22151-2388

Prof. Adam Dziewonski
Hoffman Laboratory, Harvard University
Dept. of Earth Atmos. & Planetary Sciences
20 Oxford Street
Cambridge, MA 02138

Prof. John Ebel
Department of Geology & Geophysics
Boston College
Chestnut Hill, MA 02167

Eric Fielding
SNEE Hall
INSTOC
Cornell University
Ithaca, NY 14853

Dr. Mark D. Fisk
Mission Research Corporation
735 State Street
P.O. Drawer 719
Santa Barbara, CA 93102

Prof Stanley Flatte
Applied Sciences Building
University of California, Santa Cruz
Santa Cruz, CA 95064

Dr. John Foley
NER-Geo Sciences
1100 Crown Colony Drive
Quincy, MA 02169

Prof. Donald Forsyth
Department of Geological Sciences
Brown University
Providence, RI 02912

Dr. Art Frankel
U.S. Geological Survey
922 National Center
Reston, VA 22092

Dr. Cliff Frolich
Institute of Geophysics
8701 North Mopac
Austin, TX 78759

Dr. Holly Given
IGPP, A-025
Scripps Institute of Oceanography
University of California, San Diego
La Jolla, CA 92093

Dr. Jeffrey W. Given
SAIC
10260 Campus Point Drive
San Diego, CA 92121

Dr. Dale Glover
Defense Intelligence Agency
ATTN: ODT-1B
Washington, DC 20301

Dan N. Hagedon
Pacific Northwest Laboratories
Battelle Boulevard
Richland, WA 99352

Dr. James Hannon
Lawrence Livermore National Laboratory
P.O. Box 808
L-205
Livermore, CA 94550

Prof. David G. Harkrider
Seismological Laboratory
Division of Geological & Planetary Sciences
California Institute of Technology
Pasadena, CA 91125

Prof. Danny Harvey
CIRES
University of Colorado
Boulder, CO 80309

Prof. Donald V. Helmberger
Seismological Laboratory
Division of Geological & Planetary Sciences
California Institute of Technology
Pasadena, CA 91125

Prof. Eugene Herrin
Institute for the Study of Earth and Man
Geophysical Laboratory
Southern Methodist University
Dallas, TX 75275

Prof. Robert B. Herrmann
Department of Earth & Atmospheric Sciences
St. Louis University
St. Louis, MO 63156

Prof. Lane R. Johnson
Seismographic Station
University of California
Berkeley, CA 94720

Prof. Thomas H. Jordan
Department of Earth, Atmospheric &
Planetary Sciences
Massachusetts Institute of Technology
Cambridge, MA 02139

Prof. Alan Kafka
Department of Geology & Geophysics
Boston College
Chestnut Hill, MA 02167

Robert C. Kemerait
ENSCO, Inc.
445 Pineda Court
Melbourne, FL 32940

Dr. Karl Koch
Institute for the Study of Earth and Man
Geophysical Laboratory
Southern Methodist University
Dallas, Tx 75275

Dr. Max Koontz
U.S. Dept. of Energy/DP 5
Forrestal Building
1000 Independence Avenue
Washington, DC 20585

Dr. Richard LaCoss
MIT Lincoln Laboratory, M-200B
P.O. Box 73
Lexington, MA 02173-0073

Dr. Fred K. Lamb
University of Illinois at Urbana-Champaign
Department of Physics
1110 West Green Street
Urbana, IL 61801

Prof. Charles A. Langston
Geosciences Department
403 Deike Building
The Pennsylvania State University
University Park, PA 16802

Jim Lawson, Chief Geophysicist
Oklahoma Geological Survey
Oklahoma Geophysical Observatory
P.O. Box 8
Leonard, OK 74043-0008

Prof. Thorne Lay
Institute of Tectonics
Earth Science Board
University of California, Santa Cruz
Santa Cruz, CA 95064

Dr. William Leith
U.S. Geological Survey
Mail Stop 928
Reston, VA 22092

Mr. James F. Lewkowicz
Phillips Laboratory/GPEH
29 Randolph Road
Hanscom AFB, MA 01731-3010(2 copies)

Mr. Alfred Lieberman
ACDA/VI-OA State Department Building
Room 5726
320-21st Street, NW
Washington, DC 20451

Prof. L. Timothy Long
School of Geophysical Sciences
Georgia Institute of Technology
Atlanta, GA 30332

Dr. Randolph Martin, III
New England Research, Inc.
76 Olcott Drive
White River Junction, VT 05001

Dr. Robert Masse
Denver Federal Building
Box 25046, Mail Stop 967
Denver, CO 80225

Dr. Gary McCartor
Department of Physics
Southern Methodist University
Dallas, TX 75275

Prof. Thomas V. McEvilly
Seismographic Station
University of California
Berkeley, CA 94720

Dr. Art McGarr
U.S. Geological Survey
Mail Stop 977
U.S. Geological Survey
Menlo Park, CA 94025

Dr. Keith L. McLaughlin
S-CUBED
A Division of Maxwell Laboratory
P.O. Box 1620
La Jolla, CA 92038-1620

Stephen Miller & Dr. Alexander Florence
SRI International
333 Ravenswood Avenue
Box AF 116
Menlo Park, CA 94025-3493

Prof. Bernard Minster
IGPP, A-025
Scripps Institute of Oceanography
University of California, San Diego
La Jolla, CA 92093

Prof. Brian J. Mitchell
Department of Earth & Atmospheric Sciences
St. Louis University
St. Louis, MO 63156

Mr. Jack Murphy
S-CUBED
A Division of Maxwell Laboratory
11800 Sunrise Valley Drive, Suite 1212
Reston, VA 22091 (2 Copies)

Dr. Keith K. Nakanishi
Lawrence Livermore National Laboratory
L-025
P.O. Box 808
Livermore, CA 94550

Prof. John A. Orcutt
IGPP, A-025
Scripps Institute of Oceanography
University of California, San Diego
La Jolla, CA 92093

Prof. Jeffrey Park
Kline Geology Laboratory
P.O. Box 6666
New Haven, CT 06511-8130

Dr. Howard Patton
Lawrence Livermore National Laboratory
L-025
P.O. Box 808
Livermore, CA 94550

Dr. Frank Pilotte
HQ AFTAC/TT
130 South Highway A1A
Patrick AFB, FL 32925-3002

Dr. Jay J. Pulli
Radix Systems, Inc.
201 Perry Parkway
Gaithersburg, MD 20877

Dr. Robert Reinke
ATTN: FCTVTD
Field Command
Defense Nuclear Agency
Kirtland AFB, NM 87115

Prof. Paul G. Richards
Lamont-Doherty Geological Observatory
of Columbia University
Palisades, NY 10964

Mr. Wilmer Rivers
Teledyne Geotech
314 Montgomery Street
Alexandria, VA 22314

Dr. Alan S. Ryall, Jr.
ARPA/NMRO
3701 North Fairfax Drive
Arlington, VA 22209-1714

Dr. Richard Sailor
TASC, Inc.
55 Walkers Brook Drive
Reading, MA 01867

Prof. Charles G. Sammis
Center for Earth Sciences
University of Southern California
University Park
Los Angeles, CA 90089-0741

Prof. Christopher H. Scholz
Lamont-Doherty Geological Observatory
of Columbia University
Palisades, NY 10964

Dr. Susan Schwartz
Institute of Tectonics
1156 High Street
Santa Cruz, CA 95064

Secretary of the Air Force
(SAFRD)
Washington, DC 20330

Office of the Secretary of Defense
DDR&E
Washington, DC 20330

Thomas J. Sereno, Jr.
Science Application Int'l Corp.
10260 Campus Point Drive
San Diego, CA 92121

Dr. Michael Shore
Defense Nuclear Agency/SPSS
6801 Telegraph Road
Alexandria, VA 22310

Dr. Robert Shumway
University of California Davis
Division of Statistics
Davis, CA 95616

Dr. Matthew Sibol
Virginia Tech
Seismological Observatory
4044 Derring Hall
Blacksburg, VA 24061-0420

Prof. David G. Simpson
IRIS, Inc.
1616 North Fort Myer Drive
Suite 1050
Arlington, VA 22209

Donald L. Springer
Lawrence Livermore National Laboratory
L-025
P.O. Box 808
Livermore, CA 94550

Dr. Jeffrey Stevens
S-CUBED
A Division of Maxwell Laboratory
P.O. Box 1620
La Jolla, CA 92038-1620

Lt. Col. Jim Stobie
ATTN: AFOSR/NL
110 Duncan Avenue
Bolling AFB
Washington, DC 20332-0001

Prof. Brian Stump
Institute for the Study of Earth & Man
Geophysical Laboratory
Southern Methodist University
Dallas, TX 75275

Prof. Jeremiah Sullivan
University of Illinois at Urbana-Champaign
Department of Physics
1110 West Green Street
Urbana, IL 61801

Prof. L. Sykes
Lamont-Doherty Geological Observatory
of Columbia University
Palisades, NY 10964

Dr. David Taylor
ENSCO, Inc.
445 Pineda Court
Melbourne, FL 32940

Dr. Steven R. Taylor
Los Alamos National Laboratory
P.O. Box 1663
Mail Stop C335
Los Alamos, NM 87545

Prof. Clifford Thurber
University of Wisconsin-Madison
Department of Geology & Geophysics
1215 West Dayton Street
Madison, WS 53706

Prof. M. Nafi Toksoz
Earth Resources Lab
Massachusetts Institute of Technology
42 Carleton Street
Cambridge, MA 02142

Dr. Larry Turnbull
CIA-OSWR/NED
Washington, DC 20505

Dr. Gregory van der Vink
IRIS, Inc.
1616 North Fort Myer Drive
Suite 1050
Arlington, VA 22209

Dr. Karl Veith
EG&G
5211 Auth Road
Suite 240
Suitland, MD 20746

Prof. Terry C. Wallace
Department of Geosciences
Building #77
University of Arizona
Tuscon, AZ 85721

Dr. Thomas Weaver
Los Alamos National Laboratory
P.O. Box 1663
Mail Stop C335
Los Alamos, NM 87545

Dr. William Wortman
Mission Research Corporation
8560 Cinderbed Road
Suite 700
Newington, VA 22122

Prof. Francis T. Wu
Department of Geological Sciences
State University of New York
at Binghamton
Vestal, NY 13901

ARPA, OASB/Library
3701 North Fairfax Drive
Arlington, VA 22203-1714

HQ DNA
ATTN: Technical Library
Washington, DC 20305

Defense Intelligence Agency
Directorate for Scientific & Technical Intelligence
ATTN: DTIB
Washington, DC 20340-6158

Defense Technical Information Center
Cameron Station
Alexandria, VA 22314 (2 Copies)

TACTEC
Battelle Memorial Institute
505 King Avenue
Columbus, OH 43201 (Final Report)

Phillips Laboratory
ATTN: XPG
29 Randolph Road
Hanscom AFB, MA 01731-3010

Phillips Laboratory
ATTN: GPE
29 Randolph Road
Hanscom AFB, MA 01731-3010

Phillips Laboratory
ATTN: TSML
5 Wright Street
Hanscom AFB, MA 01731-3004

Phillips Laboratory
ATTN: PL/SUL
3550 Aberdeen Ave SE
Kirtland, NM 87117-5776 (2 copies)

Dr. Michel Bouchon
I.R.I.G.M.-B.P. 68
38402 St. Martin D'Heres
Cedex, FRANCE

Dr. Michel Campillo
Observatoire de Grenoble
I.R.I.G.M.-B.P. 53
38041 Grenoble, FRANCE

Dr. Kin Yip Chun
Geophysics Division
Physics Department
University of Toronto
Ontario, CANADA

Prof. Hans-Peter Harjes
Institute for Geophysic
Ruhr University/Bochum
P.O. Box 102148
4630 Bochum 1, GERMANY

Prof. Eystein Husebye
NTNF/NORSAR
P.O. Box 51
N-2007 Kjeller, NORWAY

David Jepsen
Acting Head, Nuclear Monitoring Section
Bureau of Mineral Resources
Geology and Geophysics
G.P.O. Box 378, Canberra, AUSTRALIA

Ms. Eva Johannisson
Senior Research Officer
FOA
S-172 90 Sundbyberg, SWEDEN

Dr. Peter Marshall
Procurement Executive
Ministry of Defense
Blacknest, Brimpton
Reading FG7-FRS, UNITED KINGDOM

Dr. Bernard Massinon, Dr. Pierre Mechler
Societe Radiomana
27 rue Claude Bernard
75005 Paris, FRANCE (2 Copies)

Dr. Svein Mykkeltveit
NTNT/NORSAR
P.O. Box 51
N-2007 Kjeller, NORWAY (3 Copies)

Prof. Keith Priestley
University of Cambridge
Bullard Labs, Dept. of Earth Sciences
Madingley Rise, Madingley Road
Cambridge CB3 OEZ, ENGLAND

Dr. Jorg Schlittenhardt
Federal Institute for Geosciences & Nat'l Res.
Postfach 510153
D-30631 Hannover , GERMANY

Dr. Johannes Schweitzer
Institute of Geophysics
Ruhr University/Bochum
P.O. Box 1102148
4360 Bochum 1, GERMANY

Trust & Verify
VERTIC
8 John Adam Street
London WC2N 6EZ, ENGLAND